SYNCHROTRON RADIATION HEATING OF THE HELICAL SUPERCONDUCTING UNDULATOR*

J. Dooling†, R. Dejus, V. Sajaev, Argonne National Laboratory, Lemont, USA

Abstract

A helical superconducting undulator (HSCU) was installed in the Advanced Photon Source (APS) Storage Ring (SR) during the January 2018 maintenance period. Shortly after the reintroduction of beam into the SR in late January, higher than expected heating was observed in the cryogenic cooling system. Steering the electron beam orbit in the upstream dipole reduced the amount of synchrotron radiation reaching into the HSCU and allowed the device to properly cool and operate. Modeling the HSCU geometry with MARS shows the importance of Compton Scattering in transferring synchrotron photons with energies in the range of 10-100 keV through the vacuum chamber into the HSCU magnet pole and winding regions. Simulations carried out using MARS with EGS5 enabled indicate a rapid increase in transfer efficiency from the chamber wall to the HSCU with photon energy. Realistic spectral distributions of synchrotron photons are employed as input to MARS for several bending magnet field strengths.

INTRODUCTION

Planar superconducting undulators previously installed at APS [1] have cold vacuum chambers with large horizontal gaps, which allow shielding the chamber from the synchrotron radiation coming from the upstream dipole using radiation absorbers placed immediately in front of the SCU chamber. Unlike planar SCUs, the helical superconducting undulator (HSCU) [2] has a small vacuum chamber gap in horizontal plane that cannot be shielded from the radiation of the upstream dipole without further restricting the already-small horizontal aperture. The expected heating of the vacuum chamber due to synchrotron radiation from the upstream bending magnet was calculated and tested with the previously installed mock up chamber, based on which the HSCU cooling system was designed to handle the expected vacuum chamber heating. The HSCU was installed in Sector 7 of the APS Storage Ring (SR) during the January 2018 Maintenance period. After injecting the first electron beam, an unexpected heating of the magnet coils was observed, while the vacuum chamber temperature was at the expected level [3]. Based on the helium temperature rise, the additional head deposition was estimated to be 1 W. The heating was the same for different fill patterns, which ruled out resistive wall or wakefield effects and pointed to synchrotron radiation [4].
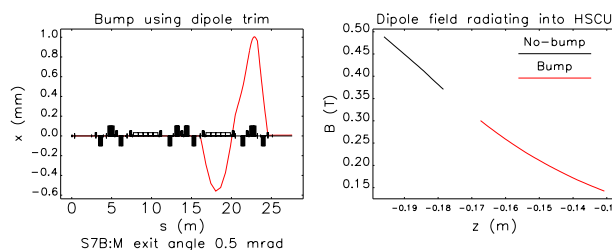

Figure 1: Left: Orbit bump that generates positive orbit angle at the exit of the dipole (one lattice sector is shown). Right: Dipole field along the beam trajectory in the dipole showing only the regions radiating into the HSCU chamber. The left-most ends of the regions radiate onto the upstream end of the chamber.

To reduce the amount of synchrotron radiation reaching into the HSCU vacuum chamber, the beam orbit was steered in the upstream bending magnet in order to generate positive horizontal orbit angle at the exit of the dipole [5]. This allows for more radiation from the end of the bending magnet to be intercepted upstream of the HSCU. Figure 1 (left) shows an orbit bump that provides a 0.5-mrad orbit angle at the dipole exit while maintaining relatively small orbit, with the disturbance confined to the downstream half of the lattice sector. This orbit bump allowed to reduce the temperature of the coils to the level compatible with the HSCU operation.

Synchrotron radiation can deposit power in the magnet coils in two ways. First, the synchrotron radiation directly strikes the vacuum chamber; the heat deposited in the chamber is then transferred to the magnet through thermal radiation. Second, the synchrotron radiation may pass through the vacuum chamber and directly strike the magnet coils. The latter seems to be less likely since the incident angle of the radiation on the vacuum chamber is about 1.5 mrad, which results in a ~1-m path length through the 1.5-mm-thick aluminum vacuum chamber.

To study the reason for the coil heating, a bump amplitude scan was performed while recording the vacuum chamber and magnet coil temperatures. Both vacuum chamber and magnet coil temperatures showed clear dependence on the bump amplitude. However, under some bump conditions, the magnet temperature was changing while the vacuum chamber temperature stayed constant. This observation clearly showed that the magnet temperature did not depend on the vacuum chamber temperature and allowed us to rule out heat transmission from the vacuum chamber to the magnet through thermal radiation as the source of the unexpected magnet heating.

† jcdooling@anl.gov

To understand how the synchrotron radiation power gets through the vacuum chamber, the bending magnet field on the part of the orbit from which the radiation is emitted into the HSCU vacuum chamber was calculated. APS bending magnets have a magnetic field of 0.6 T. The radiation that reaches into the HSCU vacuum chamber is emitted from the downstream edge of the magnet. Ray tracing was used to find the part of the orbit that emits into the HSCU vacuum chamber, then the measured field map was used to calculate the corresponding magnetic field. Figure 1 (right) shows the results of this calculation. One can see that the orbit bump lowers the magnetic field radiating into the chamber from 0.53 T to 0.35 T, which lowers the critical photon energy from 17 to 11 keV. The bending fields that the beam encounters inside quadrupoles and correctors were also checked and found to be much weaker than the field in the dipole. Using the fields shown in Fig. 1 (right), the total power radiated into the chamber for 100 mA beam current was found to be 20 W without the bump and 10 W with the bump.

A review of relevant photon interaction cross sections in the energy range of 10-100 keV and modeling the HSCU geometry with MARS showed the importance of Compton Scattering (CS) in transferring synchrotron photon energy through the vacuum chamber into the magnet pole and winding region. CS in this energy range can result in high-angle events that significantly reduce the path length of scattered photons through the vacuum chamber. Photon attenuation cross sections as a function of energy for various processes (including CS) and materials can be found in Ref. [6].

Below we present simulations of HSCU heating carried out using MARS [7–9] with EGS5 enabled. Realistic spectral distributions of synchrotron photons are employed as input to MARS for several source magnetic field intensities. Spatially, the synchrotron radiation is modeled as a pencil beam striking the center of the HSCU vacuum chamber with a horizontal angle of 1.38 mrad. We are only interested here in energy transfer; therefore, a more accurate representation of the beam spatial distribution is not required.

ANALYSIS

A. H. Compton derived the wavelength shift as a photon scatters from a single stationary electron [10]. In terms of photon energy, this shift can be expressed as

$$E_p' = \frac{E_p}{1 + \frac{E_p}{m_e c^2}(1 - \cos(\theta))}, \qquad (1)$$

where E_p and E_p' are the initial and final photon energies, h is Planck's constant, and θ is the scattering angle. For example, letting $E_p = 60$ keV and $E_p' = 59$ keV, one can find $\theta = 31.2°$ which is much larger than the incidence angle $x_o' = 0.08°$ (1.38 mrad). In this case, a photon with almost the same energy can be quickly scattered out of the 1.5-mm-thick aluminum vacuum chamber (attenuation length is ~1 cm for 50-keV photons).

Klein and Nishina published a derivation of Eq. (1) using quantum mechanics. The Klein-Nishina differential scatter-
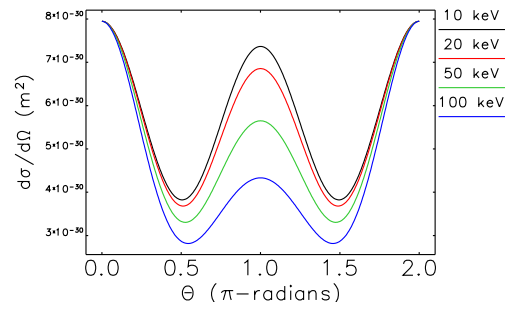

Figure 2: Differential Compton Scattering cross sections vs. angle for relevant energies in the APS SR.

ing cross section for CS from a single stationary electron may be expressed as [11]

$$\frac{d\sigma}{d\Omega} = \frac{\alpha^2 r_c^2}{2} P^2(E_p, \theta) \left[P(E_p, \theta) + P^{-1}(E_p, \theta) - \sin^2(\theta) \right] \qquad (2)$$

where Ω is the solid angle, α is the fine structure constant, $r_c = \hbar/m_e c$ is the reduced Compton wavelength, and $P(E_p, \theta)$ is the ratio of photon energy after interaction to that before the interaction that can be easily found from the expression (1). For photon energies of interest in the APS, the scattering cross section versus angle is plotted in Fig. 2. Figure 2 shows that for photon energies between 10 and 100 keV, Compton scattering generates a broad angular distribution of photons.

MARS SIMULATIONS

A point beam bending magnet model was employed to generate synchrotron photon distributions. Figure 3 presents the synchrotron spectra generated by an APS SR bending magnet at four different magnetic field intensities; these distributions were used as input to MARS. The field values represent the nominal dipole strength (0.60 T) as well as three values along the beam trajectory radiating into the chamber (0.52, 0.35, and 0.20 T) [5].

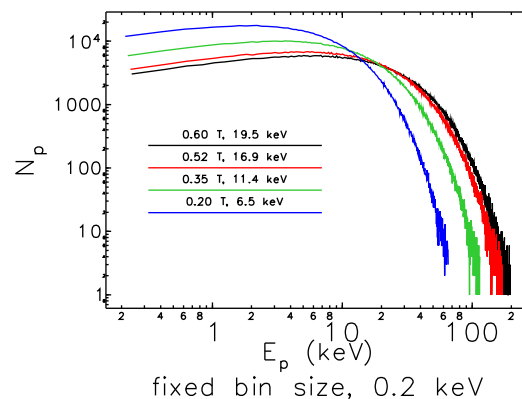Each distribution is based on one million macro-particles (photons).

Figure 3: APS SR BM synchrotron spectra for B_y=0.6, 0.52, 0.35, and 0.2 T employed as input for MARS simulations.

MC7: Accelerator Technology

T10 Superconducting Magnets

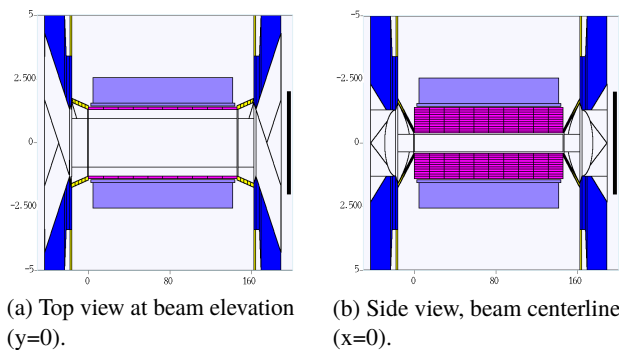(a) Top view at beam elevation (y=0).

(b) Side view, beam centerline (x=0).

Figure 4: HSCU MARS geometry. The central regions show the vacuum chamber (purple) and magnet (light blue).

(a) x-z distribution integrated across the geometry.

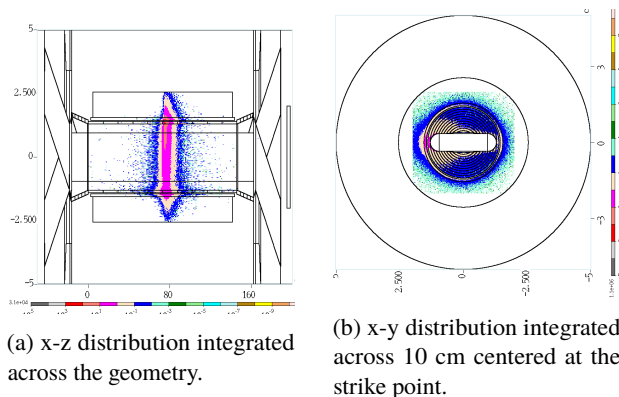(b) x-y distribution integrated across 10 cm centered at the strike point.

Figure 5: Energy deposition in the HSCU.

The MARS geometry is presented in Fig. 4. Synchrotron photons enter the geometry as a beam on the left side of Fig. 4a with an angle of $x_o' = 1.38$ mrad and a horizontal offset such that the beam strikes the outboard chamber wall centered in z along the chamber length at beam elevation ($y_o' = 0$). To improve statistics, the macro-particle input file is read five times to obtain 5 million initial photons.

Energy deposition distributions in the magnet and chamber regions are given in Fig. 5. Significant streaming of photons to the magnet region can be observed. Because of the assumption of a pencil beam rather than a distributed fan, the flux and energy deposition distributions are likely to be unrealistic; however, this work is meant only to determine the total amount of energy reaching the HSCU magnet windings. In this case, the spatial distributions are unimportant and are shown only to illustrate that a significant fraction of scattered synchrotron radiation is absorbed by the magnet. The spectra of photons streaming out of the vacuum chamber region is presented in Fig. 6.

The transverse dose distribution in Fig. 5b shows that virtually all of the energy is absorbed in the chamber and magnet regions. The amount of the absorbed power for the photon spectra plotted in Fig. 3 are presented in Table 1. The power absorbed in the magnet region versus magnetic field is shown in Fig. 7.
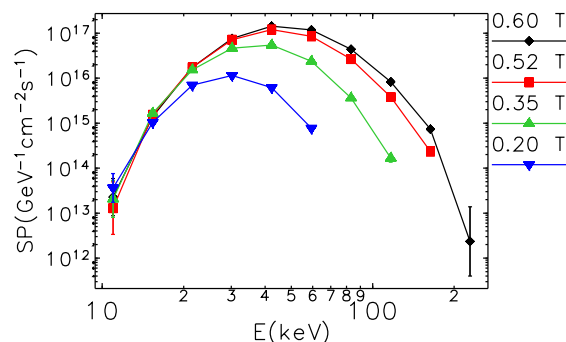

Figure 6: Spectra of photons streaming out of the aluminum vacuum chamber.

Table 1: Power Deposition (W) in the HSCU chamber and magnet for the geometry shown in Fig. 4. The magnet region is assumed to be iron.

B_y (T)	0.20	0.35	0.52	0.60
Al	6.290	10.287	13.657	14.861
Fe	0.088	0.872	2.911	4.207
Total	6.378	11.159	16.568	19.067
%Fe	1.38	7.81	17.57	22.06

SUMMARY

Simulations with MARS show that significant amounts of synchrotron radiation can be scattered into the HSCU magnet region depending on the average energy of the photons. The principle transfer mechanism for energies relevant to the APS SR is Compton scattering. These power levels are consequential to operation of the HSCU as well as the SR. Simulations also show that lowering the average photon energy (e.g., by steering the electron beam) is an effective method to reduce the fraction of Compton-scattered power reaching the magnet, as observed experimentally.
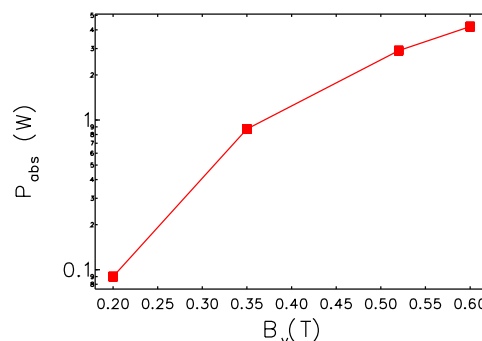
Figure 7: Comparison of absorbed energy in the magnet.

THPTS093

MC7: Accelerator Technology

T10 Superconducting Magnets

REFERENCES

[1] Y. Ivanyushenkov *et al.*, "Development and operating experience of a 1.1-m-long superconducting undulator at the advanced photon source." Phys. Rev. Accel. Beams, 20:100701, Oct 2017.

[2] M. Kasa *et al.*, "Design, construction, and magnetic field measurements of a helical superconducting undulator for the Advanced Photon Source." Proc. IPAC 2018, TUPMF008, 2018.

[3] K. Harkay, Private Communication, January 20, 2018.

[4] M. Borland, Private Communication, January 20, 2018.

[5] V. Sajaev and L. Emery, Private communication, February 6, 2018.

[6] NIST How to run the XCOM program, `https://physics.nist.gov/PhysRefData/Xcom/Text/chap4.html`

[7] N.V. Mokhov, "The Mars Code System User's Guide", Technical Note, Fermilab-FN-628 (1995).

[8] N.V. Mokhov, S.I. Striganov, "MARS15 Overview", Fermilab-Conf-07/008-AD (2007); in Proc. of Hadronic Shower Simulation Workshop, Fermilab, September 2006, AIP Conf. Proc. 896, pp. 50-60 (2007).

[9] N.V. Mokhov, P. Aarnio, Yu. Eidelman, K. Gudima, A. Konobeev, V. Pronskikh, I. Rakhno, S. Striganov, and I. Tropin, "MARS15 code developments driven by the intensity frontier needs", Prog. Nucl. Sci. Technol., 4, pp. 496-501 (2014).

[10] A. H. Compton, Physical Review, 21, p. 483 (1923).

[11] Klein-Nichina Formula, `https://en.wikipedia.org/wiki/Klein\_Nishina\_formula`